Journal of the European Ceramic Society 21 (2001) 817–824

www.elsevier.com/locate/jeurceramsoc

# Influence of the microstructure on the high temperature behaviour of gel-derived SiOC glasses

J. Parmentier [a,*], G.D. Soraru [b], F. Babonneau [c]

[a] *Laboratoire des Matériaux Minéraux, ENSCMu, Université de Haute Alsace, UPRES-A 7016, 3 rue Alfred Werner, 68093 Mulhouse Cedex, France*
[b] *Dipartimento di Ingegnera dei Materiali, Università di Trento, Via Mesiano 77, I-38050- Trento, Italy*
[c] *Chimie de la Matière Condensée, Université Paris 6/CNRS, Tour 54, 4 Place Jussieu, 75252 Paris Cedex 05, France*

Received 18 May 2000; received in revised form 31 August 2000; accepted 10 September 2000

**Abstract**

Hybrid gels, made from $HSi(OEt)_3$ and $CH_3SiH(OEt)_2$, were used to produce SiOC glasses and to study their stability at high temperature. The variation of the hydrolysis ratio allowed the formation of either dense or highly porous xerogels. This difference in microstructure was maintained at 1000°C in the glassy state and influenced the stability of these materials at higher temperature. Indeed, it plays a major role on their carbothermal degradation by promoting or hindering the removal of the gaseous products in the case of porous or dense materials respectively. In the latter case, SiOC glass appears to be a suitable candidate for thermostructural applications. 

*Keywords:* Glasses; SiOC; Sol-gel processes; Stability

## 1. Introduction

Since the first attempts to introduce carbon into glass,[1] oxycarbide glasses, also called ''black glasses'', have attracted much attention due to the wide range of possible applications.[2] Indeed, these materials have potential applications as lightweight structural materials,[3] fibers or interphases, catalyst supports,[4] and anodes in lithium ion rechargeable batteries.[5]

These glasses can be considered as an anionic modification of silica glass in which two divalent O atoms are replaced by one tetravalent C atom, and the resulting formula is $SiC_xO_{2-2x}$. They are usually prepared by pyrolysis of polysiloxanes in an inert atmosphere. This processing route leads to the expected silicon oxycarbide phase plus a free carbon phase and, therefore, their composition can be described as $SiC_xO_{2-2x} + yC_{free}$.

Because some applications concern high temperature utilization, there is a strong need to understand completely their behavior at $T > 1200$°C where decomposition or oxidation of the SiOC network can take place in inert or oxidative atmosphere, respectively. In the former case, various reactions can take place.[6] At least two equilibrium reactions [(1) and (2)] can be considered to describe the carbothermal reduction of $SiO_2$ (or $SiO_{2-2x}C_x$).[7] These reactions involve the formation of gaseous species, a weight loss and a subsequent deterioration of the mechanical properties.[8]

$$SiO_2 + 3C \leftrightarrows SiC + 2CO_g \quad (1)$$

$$2SiO_2 + SiC \leftrightarrows 3SiO_g + CO_g \quad (2)$$

Moreover, it has been shown that in the temperature range between 1200 and 1400°C, the oxycarbide glass network undergoes a structural rearrangement that leads to the crystallization of nanosized β-SiC crystallites into amorphous silica.[8–10]

Many factors have been shown to affect the high temperature stability such as the composition of the oxycarbide glasses and especially the free carbon content,[11] the type of precursor used (network architecture),[12,13] the pyrolysis atmosphere and the sample size.[11] For the last two parameters, it is believed that they influence the diffusion of the gaseous species (CO and SiO) towards the surface of the sample, with the overall effect of shifting the equilibrium of reactions (1) and (2). This explanation was supported by other studies which showed that the high temperature degradation

* Corresponding author.

0955-2219/01/$ - see front matter 
PII: S0955-2219(00)00268-5

mechanism is kinetically limited,[14] controlled by diffusion and that it can be suppressed by applying a high CO pressure.[8,15]

In this paper, we report the study of a new parameter influencing the high temperature stability: the glass microstructure. Its role has been investigated on two gel-derived SiOC glasses having similar chemical composition but different porosity and specific surface area. The high temperature behavior was investigated by TG/DTA and the materials characterized for different temperatures using BET measurements, chemical analysis, SEM and $^{29}$Si MAS NMR.

## 2. Experimental

### 2.1. Synthesis

The two studied gels were prepared from a mixture of methyldiethoxysilane ($D^H$), $CH_3SiH(OEt)_2$, and triethoxysilane ($T^H$), $HSi(OEt)_3$, in a 1/1 molar ratio and using ethanol (EtOH/Si = 2) as solvent. The hydrolysis was performed drop by drop with distilled water under vigorous stirring. Two different hydrolysis ratio were used, $H_2O$/OEt = 1 and 1/5 for sample A and B respectively. The solution was then poured into test tubes which were left open for gelation. For sample A, which was hydrolyzed using a stoichiometric amount of water, a transparent gel was obtained in less than 24 h whereas 2 weeks were needed for the understoichiometric conditions (for sample B) to give a white (xero)gel. The former is obtained with a high shrinkage ($\approx$ 60%) compared to the latter ($\approx$ 20%). After drying at room temperature and then up to 110°C by steps of 20°C for 2 days each, the resulting xerogels were ground and sieved in order to obtained powders in the size range 100–350 μm. SiOC glasses were prepared by pyrolysis of these powders at 1000°C for one hour under flowing argon (100 ml/min) using a silica tubular furnace and batches of two grams each. The powders were then sieved again to separate the fine powders formed during pyrolysis [$\varnothing < 32$ μm (fine powder)] from the coarser ones [$100 < \varnothing < 350$ μm (coarse powder)].

### 2.2. Characterization

The high temperature behavior was investigated with thermogravimetric analyses on a simultaneous DTA/TG thermoanalyser (Netzsch, STA 409), equipped with an alumina tubular furnace and alumina crucibles. Experiments were performed using about 40 mg of xerogel powder under flowing argon or air (100 ml/min) and a heating rate of 10°C/min. A buoyancy correction was applied to the TG data.

Si, C, H contents of the xerogels and SiOC glasses were determined by the Service d'Analyse Elémentaire du CNRS, France. Oxygen was estimated by difference.

The FTIR analysis were performed using the KBr pellet technique in transmission mode. 64 scans were always accumulated with a Nicolet FT–IR 5DXC equipment operating with 2 cm$^{-1}$ resolution. $^{29}$Si MAS-NMR spectra were collected with a MSL300 Bruker spectrometer at 59.6 MHz. The powdered samples were put in 7 mm zirconia rotor and spun at 4 kHz. $T_1$ relaxation times were measured using a saturation recovery method and the recycle delays were set close to 5 $T_1$ to give reliable quantitative information. 2D $^1$H–$^{29}$Si heteronuclear experiments based on the cross-polarisation sequence were recorded with a contact time of 1 ms. TPPI was used for phase sensitivity with a 3-s repetition time and 256 individual experiments with 64 acquisitions.

SEM micrographs were obtained from the surface fracture of xerogel and glass samples using a Jeol JSM 6300 equipment operating at 10 kV.

Microstructural data were collected using different techniques:

- Nitrogen adsorption/desorption measurements (micrometrics equipment) for surface area and pore size distribution analysis. Nitrogen specific surface areas at 77 K were determined from a BET (Brunauer, Emmet and Teller) analysis in the $P/P_0$ range of 0.05–0.30 using a molecular cross-sectional area of 0.163 nm$^2$ and a minimum of 5 data points. The pore size (diameter) distribution was obtained from the desorption isotherm through the BJH (Barret, Joyner and Halenda) analysis.[16]
- Hg-porosimetry (Carlo Erba equipment) for apparent density and pore volume determination.
- He- Pycnometer (Micromeritics) for the "skeleton" density measurements.

## 3. Results

### 3.1. TGA

TGA, carried out on both xerogels (argon atmosphere), are shown in Fig. 1. Both samples exhibit an important weight loss (about 15%) between 300–600°C and a smaller one in the range 600 and 1000°C, in agreement with published data.[17] In the range 1000–1200°C, the samples appear stable without mass evolution. For $T > 1200$°C, only sample B exhibits a noticeable weight loss (10%) whereas sample A shows a constant weight. This different behavior is quite surprising, taking into account that both the samples have the same starting composition and are pyrolysed in the same conditions. The explanation for the high temperature instability of sample B was investigated by characterizing the xerogels and the corresponding SiOC glasses.

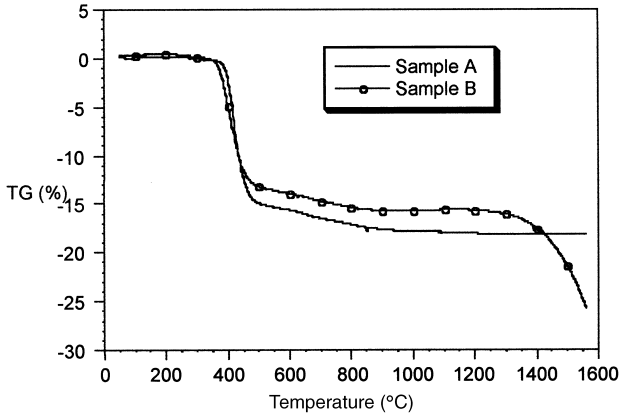


Fig. 1. DTA of xerogels A and B in argon.

### 3.2. Chemical analysis

The results of the chemical analysis performed on the starting gels and on the SiOC glasses pyrolyzed at 1000°C are reported in Table 1. The compositions of the xerogels A and B, $SiC_{0.51}O_{1.31}H_{2.37}$ and $SiC_{0.50}O_{1.37}H_{1.91}$ respectively, are quite similar and are not too far of the theoretical composition, $SiC_{0.50}O_{2.50}H_{2.50}$, of a fully condensed gel made with a ratio $T^H/D^H = 1$.

Also for the samples A and B calcined at 1000°C, their chemical compositions, $SiC_{0.42}O_{1.54}H_{0.07}$ and $SiC_{0.35}O_{1.55}H_{0.13}$ respectively, are not too far from each other. Considering that each carbon atom can replace two oxygen atoms in the silica structure, it can be re-written according to the general formula: $SiC_xO_{2-2x} + y\ C_{free}$, $SiC_{0.23}O_{1.54} + 0.19C$ and $SiC_{0.22}O_{1.55} + 0.13C$, with an excess of free carbon, as expected for the $T^H/D^H = 1$ ratio.[13]

### 3.3. FT–IR

The FT–IR spectra of the xerogels are similar to those already reported in the literature[18] and will not be presented here. Nevertheless, they show a difference of intensity between the Si–H stretching vibration peak of $T^H$ and $D^H$ units (2250 and 2180 $cm^{-1}$ respectively) suggesting a variation of $T^H/D^H$ ratio between the two samples.[18] In particular, a higher $T^H/D^H$ ratio is obtained in sample B than in A, and this could be due to a preferential evaporation of difunctional species (non-hydrolyzed or partially hydrolyzed monomers or short linear chains). This process should be more pronounced for sample B obtained using a lower hydrolysis ratio ($H_2O/OEt = 1/5$) which results into a longer gelation-drying process. The absence of absorption bands due to water shows that these materials are quite hydrophobic due to the presence of Si–H and Si–$CH_3$. Moreover, characteristic vibration bands of residuals OR or OH groups are not observed, even for sample B which was prepared using an under-stoechiometric hydrolysis ratio.

For the SiOC glasses, the main difference between the two spectra concern the presence of water (probably physisorbed) revealed by a peak at 1630 $cm^{-1}$ for sample B only, in relation to its high surface area as describe further. Both samples showed a broad band around 1890 $cm^{-1}$ which could be due to the formation of allenic structures.[19]

### 3.4. NMR

$^{29}Si$ MAS-NMR experiments were carried out on both xerogels. The $T_1$ relaxation times, chemical shift value, full width at half maximum (FWHM) and relative intensities are reported in Table 2 for each $T^H$ and $D^H$ units. Table NMR quantitative analysis show, for sample A, a $T^H/D^H$ ratio of 1/1 and for sample B a slight enrichment in $T^H$ units, in agreement with the FT–IR results.

The increase of $T_1$ and of FWHM for both $D^H$ and $T^H$ sites can be related to higher rigidity of the network in sample B. A decrease in FWHM when the $D^H/T^H$ ratio increases has already been reported[18] and assigned to an increase in the network mobility. The differences observed between samples A and B can thus be attributed to a higher $T^H/D^H$ ratio in B.

In order to know if the polymeric network of the two xerogels were structurally different, two dimensional (2D) $^1H-^{29}Si$ heteronuclear correlation experiments (HETCOR) were recorded and do not show any clear difference between both samples. Fig. 2 illustrates the result obtained for sample B. The contact time was chosen according to previous studies performed on similar gels.[20] A correlation peak is observed in both

Table 1
Chemical composition of the gel samples and Si–C–O glasses pyrolyzed at 1000°C

| Sample | Composition ( wt.%) | | | |
|---|---|---|---|---|
| | Si | C | O | H |
| A 120°C | 48.9 | 10.6 | 36.3 | 4.2 |
| B 120°C | 48.6 | 10.3 | 37.8 | 3.3 |
| A 1000°C | 48.5 | 8.8 | 42.6 | 0.1 |
| B 1000°C | 49.0 | 7.3 | 43.5 | 0.2 |

Table 2
Results of $^{29}Si$ MAS-NMR studies on xerogels A and B

| Sample | | Chemical shift (ppm) | $T_1$ (s) | FWHM (ppm) | Composition (%) |
|---|---|---|---|---|---|
| A | $D^H$ | −34.2 | 6.4 | 1.7 | 50 |
| | $T^H$ | −84.5 | 6.9 | 2.9 | 50 |
| B | $D^H$ | −34.3 | 9.7 | 2.4 | 40 |
| | $T^H$ | −84.9 | 15.4 | 3.5 | 60 |

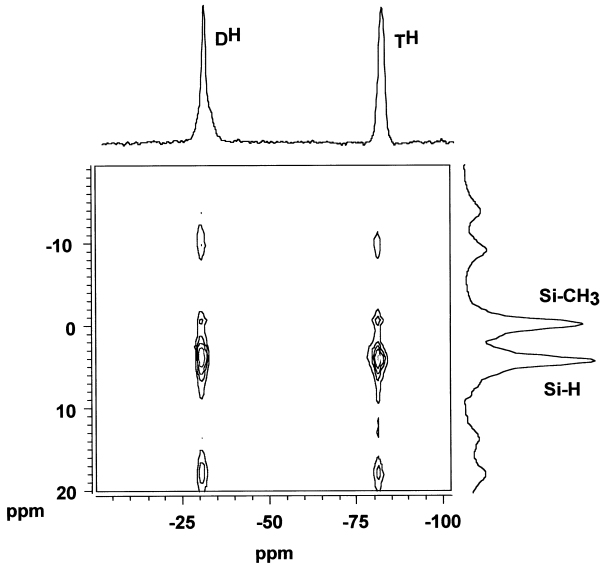


Fig. 2. $^{1}H$–$^{29}Si$ HETCOR experiments of both xerogels A and B.

gels between the protons of the methyl groups and the $T^H$ units in both samples, revealing similar homogeneous distribution of $T^H$ and $D^H$ unit , consistent with a large number of co-condensed units.

### 3.5. Microstructure

Microstructural results are reported in Table 3. One can clearly observe the difference of microstructure between the two xerogels. Sample A has a BET surface area close to zero and a very small amount of porosity (12% of the open volume by Hg-porosimetry). Moreover, this porosity has a narrow pore size distribution compare to sample B (Fig. 3). This finding is confirmed by the translucent aspect of the xerogel A. Indeed, we can say that there is only a small amount of pores or "skeleton" that have a size bigger than 1/10 of the wavelength of the visible light, i.e. above 40 nm in diameter.[21] Moreover, sample A showed a high shrinkage during the drying process (≈60%), suggesting a collapse of the gel structure with a resulting increase of the apparent density and a decrease of the surface area. On the opposite, xerogel B has a relatively high surface area (88 $m^2/g$) and a high porosity (64%). This porosity is broadly distributed, from 10 μm in diameter (Fig. 3) down to the inferior BET experimental limit (≈2 nm). Indeed, the xerogel obtained was white which means that a significant part of the pores has sizes above 40 nm. Moreover, gelation and drying occurred with a low shrinkage, suggesting that this process was not efficient regarding pore closure thus leading to a relatively high surface area and a low apparent density.

He pycnometry gave similar skeleton density (1.28 and 1.31 $g/cm^3$ for sample A and B respectively). This fact indicates that, apart from the open porosity, close porosity and/or the "packing" of the polymeric network are not too different. The similar values of skeleton density for both xerogels are in agreement with their quite close network architecture, as evidenced by MAS-NMR.

After heat-treatment at 1000°C the main microstructural differences observed for the gels were maintained in the resulting SiOC glasses. During the pyrolysis process, two competitive phenomena could take place, which led to:

- Creation of porosity due to the gas release inside the network [4] as observed for A and B in the diameter range 4–9 nm (results not shown) and evidenced by the slight increase of the surface area for sample A. Similar behaviours have already been mentioned in reference.[13]
- Closure of pores by new crosslinking reactions leading to a denser material as revealed by the decrease of the surface area of sample B.

Table 3
Summary of the microstructural results

| Technique | Type of results | Sample A | | Sample B | |
|---|---|---|---|---|---|
| | | Gel | Si–C–O glass | Gel | Si–C–O glass |
| | BET surface area ($m^2/g$) | ≈ 0 | 7.0±0.2 | 88±2 | 50±1 |
| $N_2$ ads/desorpt. | BJH desorption Cumulative pore volume ($cm^3/g$)[b] | *[a] | 0.02±0.01 | 0.45±0.02 | 0.31±0.02 |
| Hg porosimetry | Apparent density ($g/cm^3$) | 1.2±0.2 | 2.4±0.3 | 0.5±0.1 | 1.4±0.2 |
| | Total porosity (%) | 12±2 | 1±1 | 64±5 | 68±6 |
| | Cumulative pore volume ($cm^3/g$)[c] | 0.1±0.1 | ≈ 0 | 0.8±0.1 | 0.5±0.1 |
| He pycnometer | Skeleton density ($g/cm^3$) | 1.28±0.02 | 2.19±0.02 | 1.31±0.02 | 2.37±0.02 |

[a] Not performed because no accurate data could be obtained for such small surface area.
[b] For pore diameter between 2 and 300 nm.
[c] For pore diameter less than 20,000 nm.

The pore size distribution and cumulative pore volume determined by $N_2$ adsorption/desorption on glasses A and B are represented on Fig. 4.

### 3.6. SEM

SEM micrographs of both xerogels showed a smooth fracture surface for A, whereas a rough surface composed of "particles" with a diameter bellow one micron are seen for sample B (Fig. 5). These observations confirmed the results detailed previously. Sample A is a dense material compared to sample B, which is highly porous. The same features were observed for the glass samples.

### 3.7. Thermal behaviour and oxidation resistance

DTA/TGA was also performed in argon and in air on both glasses previously heat-treated at 1000°C for 1 h in argon. Two powders of different size were used: a fine one (diameter bellow 32 μm) and a coarse one ($100 < \varnothing < 350$ μm). The final weight change at 1600°C was determined from 1000°C and from room temperature for calcination in argon and air respectively. The results are reported in Table 4. The weight evolution in air is the sum of two opposite effects:

- a weight gain due to the oxidation of Si–C to Si–O bonds according to the reaction

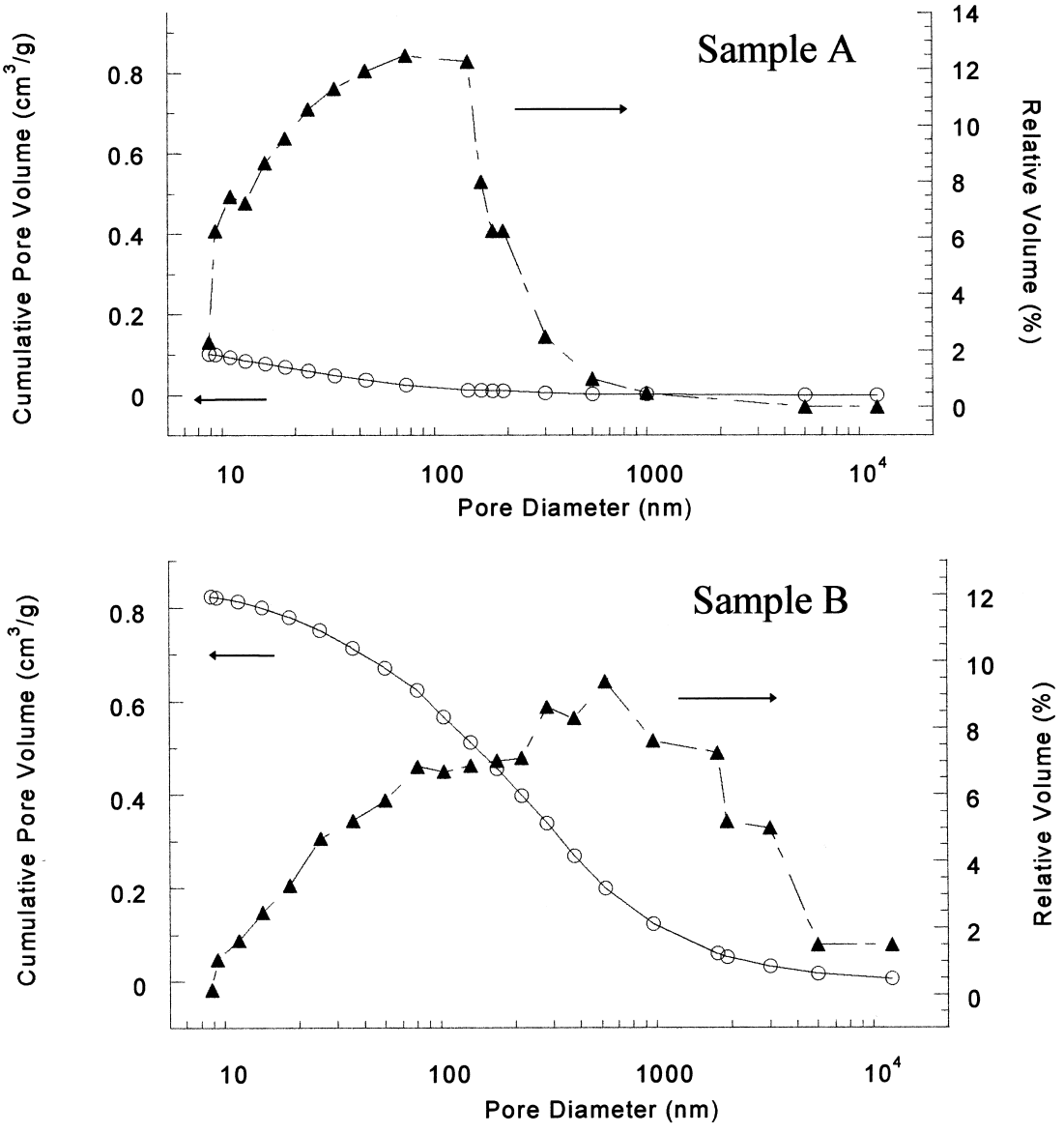


Fig. 3. Pore diameter distribution and cumulative pore volume of xerogels A and B determined by Hg-porosimetry.

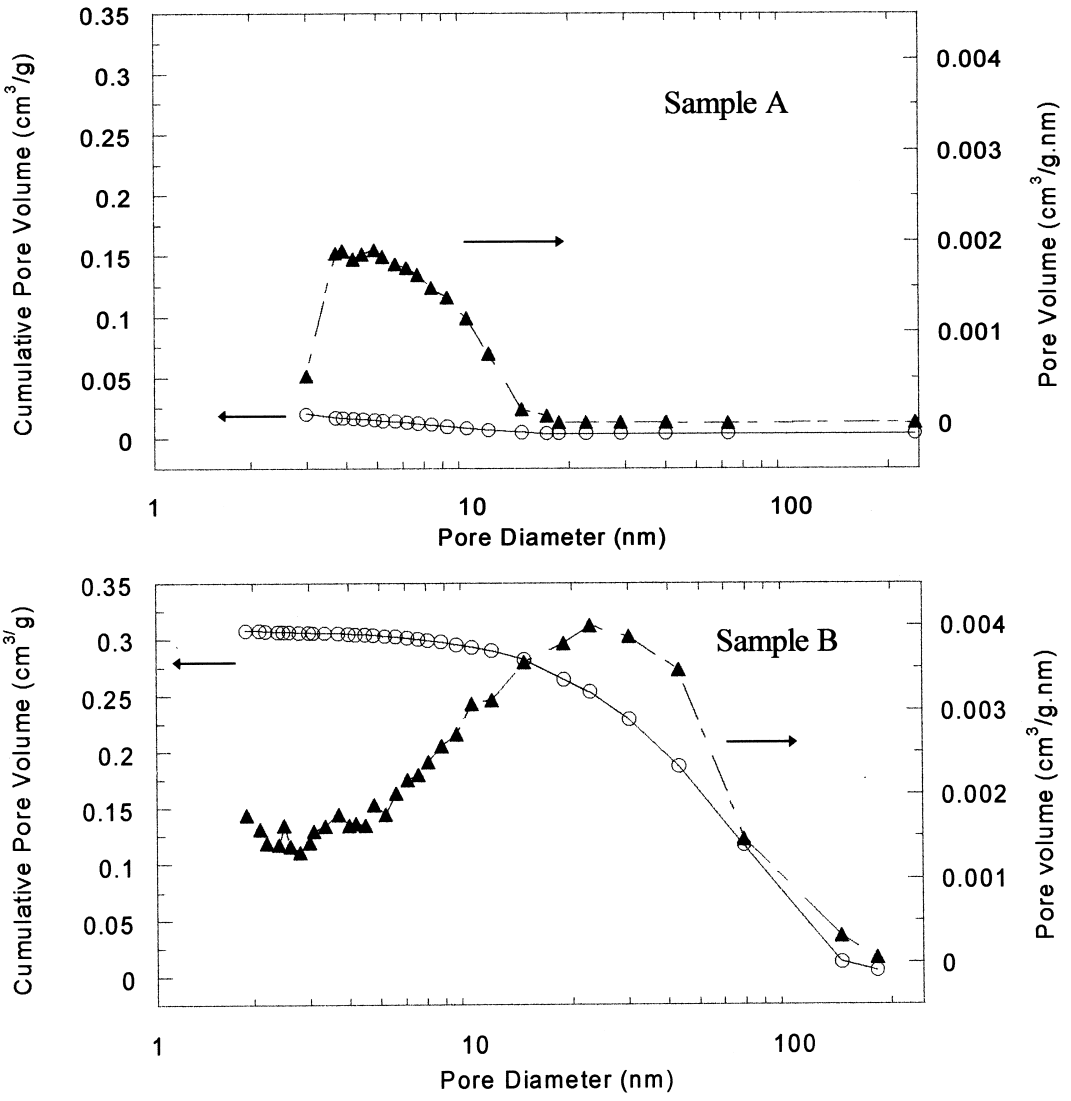


Fig. 4. Pore diameter distribution and cumulative pore volume of glasses A and B determined by $N_2$ desorption.

$$\text{Si-C-} + O_2 \rightarrow \text{Si}-\text{O}- + \text{CO}$$

- a weight loss related to the oxidation of free carbon to volatile species

$$C_{free} + O_2 \rightarrow CO_x$$

The first phenomenon took place above 500°C whereas the other one at lower temperature (≈300°C). According to the composition of glass A ($SiC_{0.23}O_{1.54}$ + 0.19C) and B ($SiC_{0.22}O_{1.55}$ + 0.13C), a complete oxidation should give an overall weight variation of +4.0 and +5.2% for A and B respectively. Experimental results (+1.1% for A and +4.9% for B) revealed that glass A indeed presents a relatively good resistance to oxidation in comparison to sample B. These results can be explained considering the higher surface area of sample B, which may enhance oxidation kinetics.

## 4. Discussion

Previous studies on the high temperature stability of SiOC glass had shown the influence of the free carbon content, polymer architecture, and particle size or heat-treatment atmosphere. In this work, the studied samples have nearly the same composition as confirmed by elementary analysis. Even if we take into account the slightly higher amount of free carbon detected for sample A, this sample should undergo the higher weight loss by carbothermal reduction. Nevertheless, the opposite behaviour is observed, sign that there are other critical parameters.

As evidenced by 2D $^{1}H$–$^{29}Si$ HETCOR MAS-NMR experiments, even the use of two quite different hydrolysis ratios ($H_2O$/OEt = 1/1 and 1/5 for sample A and B respectively), gives architectures for the resulting networks, which are very similar with no preferential phase

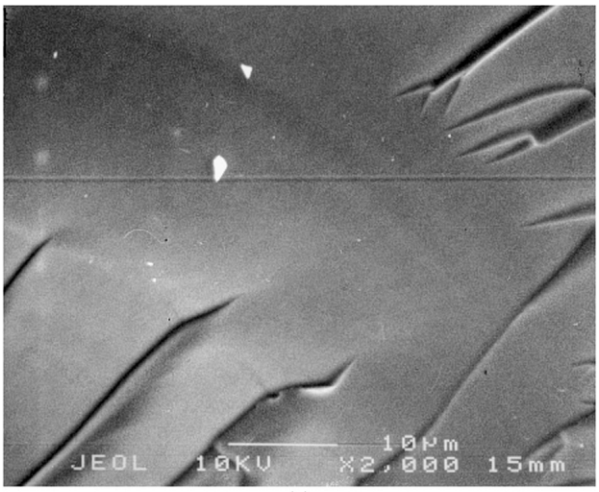


(a)

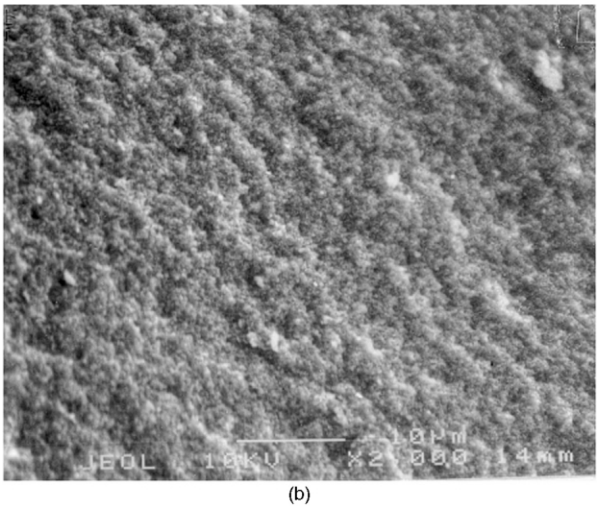


(b)

Fig. 5. SEM micrographs of fracture surface of xerogels A (a) and B (b).

Table 4
Weight change at 1600°C for glasses A and B

| Sample | Atmosphere | Weight change at 1600°C (%) | |
|---|---|---|---|
| | | Fine | Coarse |
| A | Ar | −7.1 | −0.2 |
| B | Ar | −18.1 | −9.0 |
| A | Air | – | +1.1 |
| B | Air | – | +4.9 |

separation between $D^H$ and $T^H$ units. The polymer architecture is thus not directly involved in the observed differences in high temperature behaviours.

Even the powder size and heat-treatment atmosphere cannot explain the observed differences being, all the experiments, carried out with sieved powders under the same atmosphere. Therefore, a new parameter must be introduced to explain the high temperature behaviour of SiOC glasses: the microstructure. Indeed, characterisations have shown a big difference with respect to porosity and surface area between the two xerogels; this difference was maintained at high temperature (1000°C) for the two SiOC glasses. Indeed, SiOC glass derived from sample A is non-porous with a very low surface area whereas SiOC glass derived from gel B is highly porous with a high surface area.

The thermal decomposition of the materials is promoted when the volatile products CO and SiO can be removed easily from the sample, shifting the equilibrium of the reactions (1) and (2) to the right. This condition is present with highly porous solids having a high surface area, such as sample B. On the other hand, dense SiOC glass, like sample A, does not promote the evolution of the gaseous species. The latter have to diffuse through a non-porous materials, increasing the diffusion path of the reaction products with the effects of hindering the degradation and improving its high temperature stability.

Comparison of the TGA results obtained on powders having different sizes (Table 4) shows that the high temperature stability of SiOC glasses is strongly influenced by the glass microstructure, as well as the powder size and the free carbon content. Indeed, by decreasing the powder size, the carbothermal reduction is promoted, as already shown in a previous study by Soraru et al.[11] However, it is worth noting that in our case, even with fine powders (diameter $< 32$ μm), the degradation of the material is significantly enhanced in the highly porous sample B (18% weight loss) compared to the non porous sample A (7% ) or similar sample of the literature (5%).[11]

In conclusion, by modifying just one parameter of the sol-gel process, the hydrolysis ratio, we were able to obtain materials with similar composition, close network architecture at the local scale but completely different microstructure, as determined by Hg-porosimetry, $N_2$ gas ads/desorption and SEM studies. Such a different gel microstructure was maintained into the SiOC glass and rules out its high temperature stability. It is worth noting that the high influence of the hydrolysis ratio on the microstructure was only revealed for these particular synthesis conditions. Tests done by varying other parameters such as concentration of precursors did not lead to such structural modifications. It is believed that two phenomena could explain the influence of the synthesis on the microstructure. The first one is due to different gel growth mechanisms, as described by Scherer and Brinker [21] with a cluster–cluster, and a monomer–cluster type of growth for A for B respectively. The second one related to phase separation during the gelation process are already observed in similar system.[22]

## 5. Conclusions

It has been shown that the $T^H/D^H$ system is very sensitive to the parameters used in the sol-gel processing. In some particular conditions, the simple variation of the

hydrolysis ratio leads to important modifications of the microstructure of the resulting xerogels and of the corresponding SiOC glasses. Microstructure is a new parameter, which plays a crucial role on the high temperature stability as well as other factors such as free carbon content, precursor molecular structure, powder size and atmosphere. Indeed, porosity promotes the carbothermal decomposition of the SiOC glasses by an easier removal of the volatile products shifting the equilibrium (1) and (2) towards the right. Moreover, this type of microstructure enhances oxidation reactions, in opposition to dense material. For the latter, SiOC glasses have exhibited a good thermal stability and appear as an interesting material for thermostructural applications.

## Acknowledgements

Research supported by MURST (PRIN 99) Italy, Progetto Galileo (France/Italy) and the European Commission within the framework of a TMR Network on "Oxycarbide Glasses" (FMRX-CT98-0161).

## References

1. Ellis, R. Method of making electrically conducting glass and articles made therefrom. US Patent 2,556,616, 12 June 1951.
2. Pantano, C. G., Singh, A. K. and Zhang, H., Silicon oxycarbide glasses. *J. Sol-Gel Sci.Technol*., 1999, **14**, 7–25.
3. Colombo, P. and Modesti, M., Silicon oxycarbide foams from a silicon preceramic polymer and polyurethane. *J. Sol-Gel Sci. Technol*., 1999, **14**, 103–111.
4. Singh, A. K. and Pantano, C. G., Porous silicon oxycarbide glasses. *J. Am. Ceram. Soc*., 1996, **79**, 2696–2704.
5. Xing, W., Wilson, A. M., Eguchi, K., Zank, G. A. and Dahn, J. R., Pyrolyzed polysiloxanes for use as anode materials in lithium-ion batteries. *J. Electrochem. Soc*., 1997, **144**, 2410–2416.
6. Danes, F., Saint-aman, E. and Coudurier, L., The Si–C–O system. *J. Mater. Sci*., 1993, **28**, 489–495.
7. Filsinger, D. H. and Bourrie, D. B., Silica to silicon: key carbothermic reactions and kinetics. *J. Am. Ceram. Soc*., 1990, **73**, 1726–1732.
8. Labrugere, C., Guette, A. and Naslain, R., Effect of ageing treatments at high temperatures on the microstructure and mechanical behavior of 2D Nicalon/C/SiC composites. I: ageing under vacuum or argon. *J. Eur. Ceram. Soc*., 1997, **17**, 623.
9. Soraru, G. D., D'Andrea, G., Campostrini, R., Babonneau, F. and Mariotto, G., Structural characterization and high temperature behaviour of silicon oxycarbide glasses prepared from sol-gel precursors containing Si–H bonds. *J. Am. Ceram. Soc*., 1995, **78**, 379–387.
10. Brequel, H., Parmentier, J., Soraru, G. D., Schiffini, L. and Enzo, S. Study of the phase separation in amorphous silicon oxycarbide glass under heat-treatments. *Nanostructured Materials*, in press.
11. Soraru, G. D. and Suttor, D., High temperature stability of sol-gel-derived SiOC glasses. *J. Sol-Gel Sci. Technol*., 1999, **14**, 69–74.
12. Dirè, S., Oliver, M. and Sorarù, G.D. Effect of polymer architecture on the formation of Si–O–C glasses. In *Advanced Synthesis and Processing of Composites and Advanced Ceramics II*, ed. by K. V. Logan, Z. Munir and R. M. Spriggs. *Ceramic Transactions*, 1999, 79, 251–61.
13. Sorarù, G. D., Liu, Q., Interrante, L. V. and Apple, T., The role of precursor molecolar structure on the microstructure and high temperature stability of silicon oxycarbide glasses derived from methylen-bridged polycarbosilanes. *Chem. Mater*., 1998, **10**, 4047–4054.
14. Rocabois, P., Chatillon, C. and Bernard, C., Multiple-Knudsen-cell mass spectrometry investigation of the evaporation of silicon oxycarbide glasses. *Surface and Coatings Technology*, 1993, **61**, 86–92.
15. Bibbo, G. S., Benson, P. M. and Pantano, C. G., Effect of carbon monoxide partial pressure on the high-temperature decomposition of Nicalon fibre. *J. Mater. Sci*., 5075, **26**, 1991.
16. Gregg, S. J. and Sing, K. S. W., *Adsorption, Surface Area and Porosity*. Academic Press, London, 1982.
17. Campostrini, R., D'Andrea, G., Carturan, G., Ceccato, R. and Sorarù, G. D., Pyrolysis study of methyl-substituted Si–H containing gels as precursors for oxycarbide glasses, by combined thermogravimetric, gas chromatographic and mass spectrometric analysis. *J. Mater. Chem*., 1996, **6**, 585–594.
18. Sorarù, G. D., D'Andrea, G., Campostrini, R. and Babonneau, F., Characterization of methyl-substituted silica gels with Si–H functionalities. *J. Mater. Chem*., 1995, **5**, 1363–1374.
19. Singh, A. K. and Pantano, C. G., Surface chemistry of silicon oxycarbe gels and glasses. *J. Sol-Gel Sci. Technol*., 1997, **8**, 371–376.
20. Babonneau, F. and Maquet, J., NMR techniques for the structural characterization of siloxane-oxide hybrid materials. *Polyhedron*, 2000, **19**, 315–322.
21. Jeffrey Brinker, C. and Scherer, Georege W. *Sol-Gel Sience: The Physics and Chemistry of Sol-Gel Processing*. Academic Press, Harcourt Brace Jovanovich Publishers, Boston, San Diego, New York, London, Sydney, Tokyo, Toronto. 1990.
22. Schaefer, D. W., Mark, J. E., McCarthy, D., Jian, L., Sun, C.-C. and Farago, B., Structure of microphase-separated silica-siloxane molecular composites. In *Polymer-Based Molecular Composites*, ed. D. W. Schaefer and J. E. Mark. Materials Research Society, Pittsburg, PA, 1990, pp. 57–63.